Implication of the Madden–Julian Oscillation in the 40-Day Variability of the West African Monsoon

BENJAMIN POHL

Centre de Recherches de Climatologie, CNRS/Université de Bourgogne, Dijon, France

SERGE JANICOT

LOCEAN, IRD/Université Pierre et Marie Curie, Paris, France

BERNARD FONTAINE AND ROMAIN MARTEAU

Centre de Recherches de Climatologie, CNRS/Université de Bourgogne, Dijon, France

(Manuscript received 25 August 2008, in final form 14 December 2008)

ABSTRACT

Madden–Julian oscillations (MJOs) are extracted over the Indo-Pacific basin using a local mode analysis. The convective perturbations are then projected over a larger domain to evaluate their remote consequences over the West African monsoon (WAM) intraseasonal variability. Rather weak (4–6 W m^{-2}) convective fluctuations occurring in phase with those over the southern Indian basin are found over Africa, confirming the results of Matthews. In reverse, 40-day fluctuations in the WAM, similarly detected and projected over a widened area, demonstrate that a large majority of these events are embedded in the larger-scale patterns of the MJO. The regional amplitude of intraseasonal perturbations of the West African convection is not statistically associated with the amplitude of the MJO over the Indian basin but is instead closely related to background vertical velocity anomalies over Africa, possibly embedded in changes in the regional Walker-type circulation. Subsiding motion over Africa is recorded during the most energetic convective perturbations in the WAM.

Composites analyses over the MJO life cycle, as depicted by the real-time daily indices developed by Wheeler and Hendon, show that positive outgoing longwave radiation (OLR) anomalies during the dry phase are of larger amplitude and spatially more coherent than negative anomalies during the wet phase, especially over the Sahel region. Over West Africa, the phase of suppressed convection is thus of greater importance for the region than the phase of enhanced convection. Rain gauge records fully confirm these results. The MJO appears to be significantly involved in the occurrences of dry spells during the monsoon over the Sahel, whereas large-scale convective clusters are only restricted to the equatorial latitudes and thus affect the Guinean belt, which experiences its short dry season at this time of the year.

1. Introduction

The intraseasonal variability of the West African monsoon (WAM) has been rather neglected to date, especially in comparison with the mesoscale and the synoptic time scale associated with the development of easterly waves. Janicot and Sultan (2001) and Sultan et al. (2003) identified two major periodicities in the WAM rainfall and convective variability centered on the 10–25-day range (with a peak at 15 days) and the 25–60-day range (with a peak at 38 days). The latter frequencies are clearly reminiscent of the Madden–Julian oscillation (MJO; Madden and Julian 1994; Zhang 2005), the dominant mode of intraseasonal variability in the tropical atmosphere. The MJO basically consists in an averaged eastward propagation of large-scale convective clusters (~10 000 km across) along the equator, mainly from the Indian Ocean to the Maritime Continent and then to the west Pacific. Though its convective signals are mostly restricted to the warm pool region [Indo-Pacific (IP) basin], significant anomalies can be found in most atmospheric fields (geopotential

Corresponding author address: Benjamin Pohl, Centre de Recherches de Climatologie, 6 Boulevard Gabriel, 21000 Dijon, France. E-mail: benjamin.pohl@u-bourgogne.fr

DOI: 10.1175/2009JCLI2805.1

height, temperature, and pressure) in the overall tropical belt and from the surface to the tropopause. During boreal summer, northward propagations are prevalent over the Asian sector, where the MJO significantly affects the monsoon (Yasunari 1980).

In the Western Hemisphere, Maloney and Kiehl (2002) identified MJO-related signals over the eastern Pacific basin during boreal summer, and Foltz and McPhaden (2004) depicted similar fluctuations over the tropical Atlantic basin (but mostly during northern winter and spring). The MJO was also seen to strongly modulate atmospheric convection in the South Atlantic convergence zone (Carvalho et al. 2004).

Over Africa, the associated atmospheric and convective fluctuations are not as well documented. One of the reasons is that the convective signal associated with the MJO is much weaker than over the warm pool of the Indian and west Pacific basins. The implication of the MJO in the WAM intraseasonal variability was addressed recently by Matthews (2004). Consequent to a phase of suppressed convection occurring over the warm pool region, an atmospheric Kelvin wave is propagating from the Indian Ocean along the equator toward the east and a Rossby wave is propagating over East Africa toward the west. These two waves meet 20 days later over West Africa (WA), inducing negative midtropospheric temperature anomalies that favor deep convection. Thus, a phase of suppressed convection occurs over the warm pool region 20 days before the phase of active convection over Africa. More recently, Maloney and Shaman (2008) confirmed these findings. Based on Tropical Rainfall Measuring Mission (TRMM) rainfall estimates, they pointed out that the MJO explains up to 30% of the 30–90-day variance of the rainfall in the monsoon area. Janicot et al. (2009) established that this related-MJO signal over Africa is mainly characterized by a westward propagation at the Sahel latitudes and a more stationary evolution along the Guinean coast. They estimated that the westward propagations over the Sahel originate from convectively coupled Rossby waves. In agreement with Mounier (2005), the Kelvin signal associated with the 40-day variability is found to be negligible over West Africa.

This study aims at filling some gaps concerning the implication of the MJO in the WAM intraseasonal variability and the amplitude of associated perturbations: (i) Which part of the 40-day variability of the WAM is related to the global-scale MJO activity? (ii) What is the amplitude of the MJO-associated convective fluctuations over West Africa, and which climatic parameters are associated with the variability of this amplitude? (iii) What are the consequences of the MJO on daily rain gauge records? To answer these questions we make use of two different and complementary statistical approaches to extract the MJO signal and relate it to the 40-day variability in the WAM. One of these is a novel use of a local mode analysis (LMA) that detects the intraseasonal perturbations over a given domain and allows us to quantify their influence over a remote area. The effects of the MJO on the rainfall field are examined through daily rain gauge records over the central and western Sahel, avoiding the use of satellite estimates.

The paper is organized as follows: Section 2 presents the data and methodology used to extract the MJO signal. Section 3 investigates the implication of the MJO in the 40-day variability of the WAM. Section 4 describes the outgoing longwave radiation (OLR) and rainfall anomalies over the MJO life cycle. The main results are summarized and discussed in section 5.

2. Data and methods

Tropical convection is estimated through the daily interpolated version of the OLR dataset (Liebmann and Smith 1996). It is available on a 2.5° × 2.5° regular grid from 1974, with a 10-month gap in 1978. The study period was here restricted to 1979–2007. Atmospheric circulation is examined using the National Centers for Environmental Prediction–Department of Energy (NCEP–DOE) Atmospheric Model Intercomparison Project II (AMIP-II; also referred to as NCEP-2) reanalyses (Kanamitsu et al. 2002). This study makes use of the zonal, meridional (m s^{-1}), and vertical (Pa s^{-1}) components of the wind. The velocity potential and streamfunction fields were calculated from the daily horizontal wind.

The daily rainfall data used in this study were compiled by the Flow Regimes from International Experimental and Network Data–Afrique de l'Ouest et Centrale (FRIEND-AOC) group from various sources [Institut de Recherche pour le Développement (IRD), Agence pour la Securité de la Navigation Aérienne en Afrique (ASECNA), Direction Météorologique Nationale (DMN), and Comité InterAfricain d'Etudes Hydrauliques (CIEH)]. Daily rainfall amounts recorded at 118 rain gauge stations are available over the 1950–90 period (available online at http://armspark.msem.univ-montp2.fr/FRIENDAOC/). Figure 1a shows the location of these stations: 33 in Senegal, 42 in Mali, and 43 in Burkina Faso. Thus, the dataset is useful to document the rainfall field over the central and western Sahel. Missing values are quite rare (0.67% on average) and were ignored in the following analyses. Note, however, that missing days are clearly concentrated in the years 1965–80 and from May to September (Fig. 1b). We

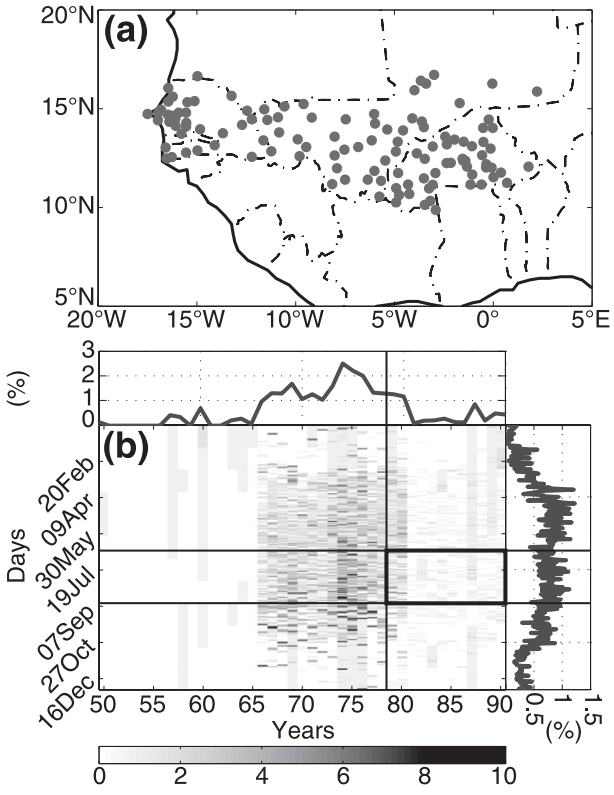

FIG. 1. (a) Location of the 118 rain gauge stations compiled in the FRIEND-AOC dataset over West Africa (Senegal, Mali, and Burkina Faso) and (b) temporal distribution of the missing values. Shadings correspond to the part of rain gauge stations (%) with missing values. Annual and seasonal means are shown in the top and right of (b), respectively. The black box in (b) shows the data used in this study.

focused here mostly on the 1979–90 period to match the OLR period.

Sea surface temperature (SST) is provided by the Reynolds et al. (2002) dataset. Weekly data were linearly interpolated at the daily time scale for the ease of computation.

The MJO signal was extracted using two complementary approaches: an LMA (Goulet and Duvel 2000; Duvel et al. 2004; Duvel and Vialard 2007) and the real-time daily indices developed by Wheeler and Hendon (2004, hereafter WH04). The LMA algorithm leads to the identification of intraseasonal events individually and documents their variability and their diversity. It is particularly adequate to focus on the propagative patterns of the MJO-associated large-scale convective disturbances. WH04 indices provide a more standard definition of the MJO. Computed on the overall tropical belt, they constitute a useful tool to compute a composite analysis depicting the average MJO life cycle and to analyze the phase locking of atmospheric anomalies between a given region and the near global-scale MJO activity.

The LMA, applied to the OLR field, is first used to extract Madden–Julian and 40-day events individually. It is based on a series of complex empirical orthogonal functions (CEOFs) performed on a short time section running along the full time series. This also generates a time series of the percentage of variance explained by the first CEOF. Local maxima in this time series correspond to convective events that are well organized at a large scale. Only the time sections centered on these events (i.e., the local modes) are retained (Fig. 2). The complex eigenvector gives the amplitude and phase of the perturbation for each region and each event, together with the time spectral characteristics. For a complex eigenvector, any relative phase between regions and thus any type of propagation may be described by a single component. With this mathematical representation of the pattern, it is possible to measure the resemblance between intraseasonal events using simple metrics (Goulet and Duvel 2000). An average pattern can be computed by performing an average complex EOF for an ensemble of local modes selected following different criteria (season, years, regional or spectral characteristics, etc.).

In the following, the LMA is performed on the OLR time series filtered in the 20–120-day band to fit the spectral features of the MJO. The length of the moving time window is 120 days and the lag between two successive positions of the time window is 5 days. Because the time series describing the percentage of variance presents some high-frequency noise, two local maxima are liable to occur within a few days, which leads to the extraction of too many local modes, or MJO events, that are not well separated from each other. Hence, we removed the overlapping local modes. Considering two successive local modes A and B characterized by their periods (in days) P_A and P_B, we calculated Δ, the number of days separating A and B, and removed the weakest of the two modes when $\Delta < \frac{P_A + P_B}{2}$ (i.e., the mode associated with the smaller percentage of variance explained by the first eigenvector).

Two different experiments are made to investigate the relationship between the convective perturbations localized over West Africa and the Madden–Julian convective perturbations in the Indian and west Pacific area.

The 40-day convective perturbations in the WAM are first detected in the filtered OLR field over the domain 0°–20°N, 20°W–35°E (i.e., the WA experiment). The local modes are then projected on a larger domain extending as far as the Indo-Pacific basin (30°N–30°S, 100°W–180°E), which constitutes a novel use of the local

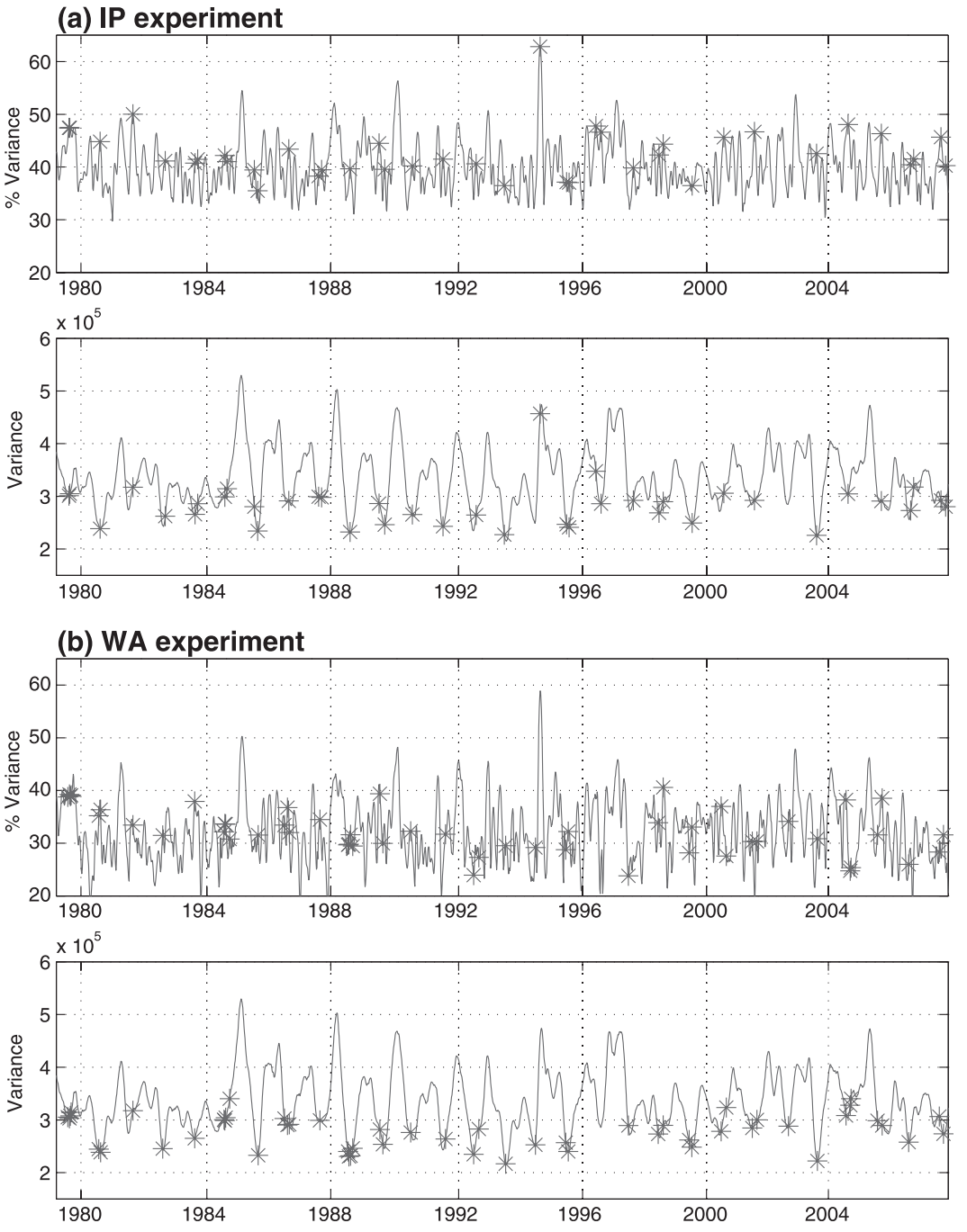

FIG. 2. (top) Percentage of variance explained by the first complex eigenvector on a 120-day-long running window for the (a) IP (5°S–20°N, 60°–160°E) and (b) WA (0°–20°N, 20°W–35°E) experiments. The stars represent local maxima in the percentage of variance, used to define the local modes. (bottom) The corresponding variance of OLR perturbations ($W^2\ m^{-4}$) for the (a) IP and (b) WA experiments.

mode analysis. Mathematically, the methodology is based on the multivariate version of the LMA presented in Duvel and Vialard (2007): the local modes are detected on a given field (OLR here) and a ''spectral key'' is used to investigate the associated signals in other fields (e.g., SST and the zonal wind). The particularity here is that we consider the same OLR field (but on a larger domain) as a second field on which the local modes are projected. This new methodology allows investigating whether the convective perturbations over West Africa

are embedded in larger-scale patterns (e.g., preceding OLR signals over Amazonia and/or following ones over the Indian Ocean basin).

Symmetrically, the Madden–Julian events in the Indo-Pacific basin (the IP experiment) are extracted with an LMA applied for the area 5°S–20°N, 60°–160°E; that is, the area over which the MJO signal is the strongest during the boreal summer season (Knutson and Weickmann 1987; Matthews 2000; Bellenger and Duvel 2007). These local modes were similarly projected on the larger domain to assess their consequences over the Western Hemisphere, particularly West Africa.

Basically, the IP experiment thus detects the Madden–Julian events and quantifies their remote amplitude over West Africa. The WA experiment extracts the 40-day variability of the WAM (Janicot and Sultan 2001; Sultan et al. 2003) and investigates whether it is embedded in larger patterns and possibly those of the MJO.

Figure 2 shows that both variance and percentage of variance reach higher values for the IP experiment, demonstrating that the signal-to-noise ratio is higher over the warm pool. It appears also clearly that the season considered in this study [July–September (JAS)] generally concentrates the weakest intraseasonal events, the peak of MJO activity being confined to boreal winter, in agreement with Salby and Hendon (1994).

LMA analyses directly applied on larger domains (e.g., the overall tropical belt) show results that are very similar to the IP experiment because the warm pool appears as the key region that triggers most of the MJO convective activity and concentrates most of its associated variance. It should also be noted that no variance threshold is retained for the selection of the events, the test that is applied to remove overlapping events ensuring that our sample is constituted of well-individualized MJO modes.

A more consensual way to depict the global-scale MJO is through the use of the real-time daily indices developed by WH04. The indices are the principal component (PC) time series of the two leading EOFs of combined daily mean tropical (averaged 15°N–15°S) 850- and 200-hPa zonal wind and OLR anomalies. WH04 subtracted the annual cycle and the low-frequency variability associated with ENSO before calculating the EOF. The indices, denoted real-time multivariate MJO 1 (RMM1) and 2 (RMM2), were designed to capture both the northern winter and summer MJO. RMM1 and RMM2 are approximately in quadrature and describe the average large-scale, eastward-propagating convective and circulation anomalies associated with the MJO. The evolution of the MJO can be concisely visualized in a two-dimensional phase-space diagram, with RMM1 and RMM2 as the horizontal and vertical Cartesian axes, respectively. A polar coordinate representation can also be used (Matthews 2000) in this phase space, where A is the amplitude of the oscillation ($A > 0$) and α is the phase angle in radians ($0 \leq \alpha \leq 2\pi$), approximately corresponding to the location of the MJO-associated convective clusters in the tropical belt. Following WH04, the MJO convection is located over the Indian Ocean at phase $3\pi/2$, Indonesia at 2π, and Africa at π. In this paper, we use both the polar and Cartesian notations of the MJO.

3. Implication of the MJO in the 40-day variability of the monsoon

a. Analysis of the local modes

To what extent is the 40-day variability of the WAM imputable to the MJO? Are all these fluctuations the regional signature of the global-scale MJO (Matthews 2004) or are some of them related to other phenomena (such as a possible intrinsic variability of the WAM)? Mounier (2005) suggested, for instance, the implication of two distinct modes of atmospheric variability to explain the 40-day fluctuations in the WAM: the MJO mode, associated with eastward propagations in the tropics and the ''global African mode'' inducing westward propagations over West Africa. To examine these questions, we compare here the results of the local modes detected in the WA and IP experiments.

Over the 1979–2007 period, the IP experiment leads to the extraction of 157 local modes (an average of 5.41 Madden–Julian events per year). Among them, 38 occurred during the JAS season (1.31 year^{-1}). The WA experiment constituted a sample of 142 local modes (4.89 year^{-1}), among which 38 occurred in JAS. Thus, each monsoon season experiences an 1.31 40-day events on average, a result intuitively coherent given the length of the season (92 days). In the following, we restricted the study period to the JAS trimester, corresponding to the development of the monsoon circulation over West Africa.

For each experiment, we compute the mean propagative pattern of the large-scale OLR perturbations (Duvel et al. 2004; Duvel and Vialard 2007), based only on the local modes recorded during JAS. The mean patterns are shown in Fig. 3, along with the regions used in each case for the detection of the local modes (see section 2). Figure 4 presents the spectral characteristics of the local modes (i.e., the distribution of the period of the events constituting each sample).

The IP experiment (Figs. 3b, 4a) extracts the well-known features of the boreal summer MJO (Lawrence and Webster 2002; Wu et al. 2006). Over the Indo-Pacific

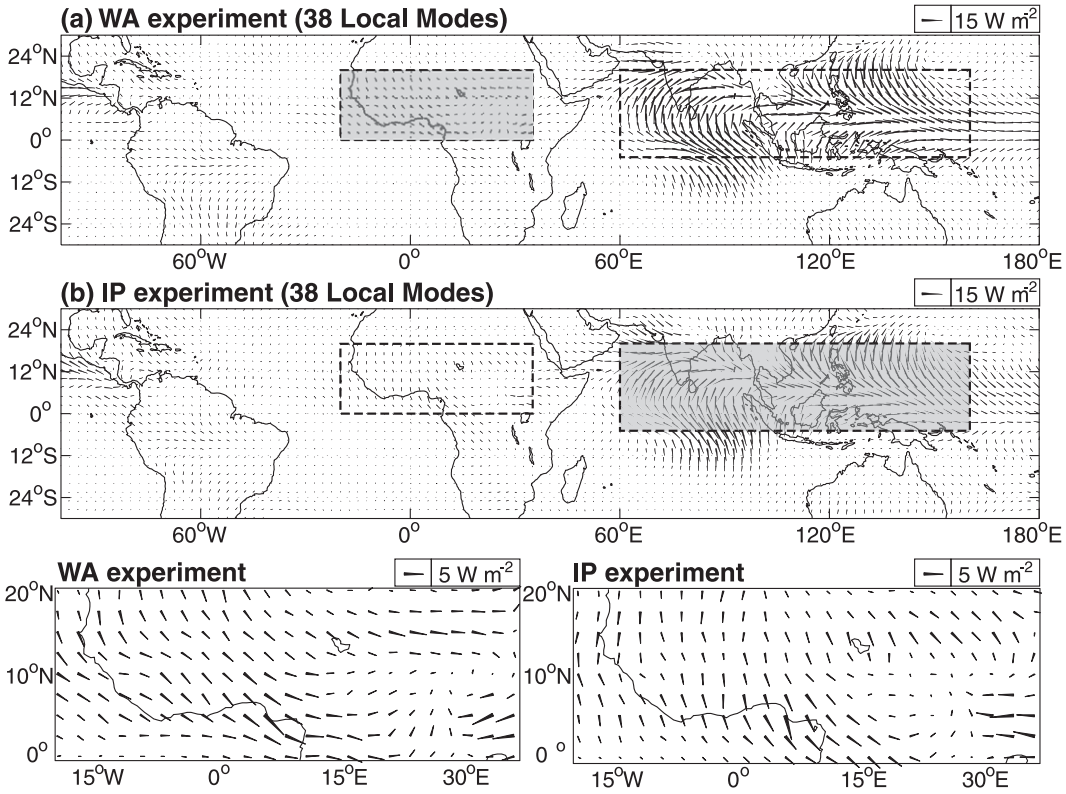

FIG. 3. The (a) WA and (b) IP experiments. See text for details. Vectors show the mean propagative pattern of OLR perturbations. The amplitude of the modes (W m^{-2}) is proportional to the segment length for each OLR grid point, and the phase at which the maximum perturbation occurs is represented as the angle of the corresponding segment. The propagation of OLR anomalies is seen as the clockwise increase of the angle with time (e.g., eastward propagation for a segment rotating clockwise toward the east). Shading represents the area used for the detection of the local modes. Dashed boxes correspond to the West Africa and Indian Ocean regional indices. (bottom) The propagative patterns over West Africa.

basin, northward propagations are prevalent, as shown by the clockwise rotation of the vectors from south to north. They are particularly marked in the Indian sector, where the convective perturbations are responsible for the intraseasonal variability of the Asian monsoon and reach the Himalaya Mountains. Westward propagations are also found in the west Pacific sector, west of the Philippines, in agreement with Wang and Xie (1997), Annamalai and Slingo (2001), and Hsu and Weng (2001). The median period of these events (Fig. 4) is 40 days, varying mostly between 36 and 46 days with extreme values at 28 and 55 days. These period values are in good agreement with the literature (e.g., Anderson et al. 1984; Madden 1986; Gray 1988; Anyamba and Weare 1995; Pohl and Matthews 2007).

Over West Africa, the amplitude of the convective perturbations is about 2 times smaller than it is farther east. The phase–amplitude vectors describe a tendency for the MJO-associated convective anomalies to propagate toward the west, from the eastern Sahel to the Atlantic coast, consistent with Janicot et al. (2009). Coherent signals, in phase with the western Sahel perturbations, are also observed over the Gulf of Guinea, although this region experiences its short dry season during the JAS trimester. Similar findings are found in Matthews (2004) and Maloney and Shaman (2008). Given the phase relationship between the West African convective signals and those located over the central Indian basin (a quarter of cycle; see the vector orientations in Fig. 3b) and given the median period of the local modes (40 days; Fig. 4a), one can conclude that the convective perturbations over the eastern Sahel lead those over the Indian Ocean by 10 days. Such a result is fully compatible with Matthews (2004, see his Fig. 4) and depicts the decaying phase of an MJO event initiated between 20 and 30 days earlier over the Indian Ocean. Hence, the westward propagations over the Sahel could be due to the Rossby wave generated by this convective disturbance, which propagates from the Indian Ocean toward the west, over tropical Africa.

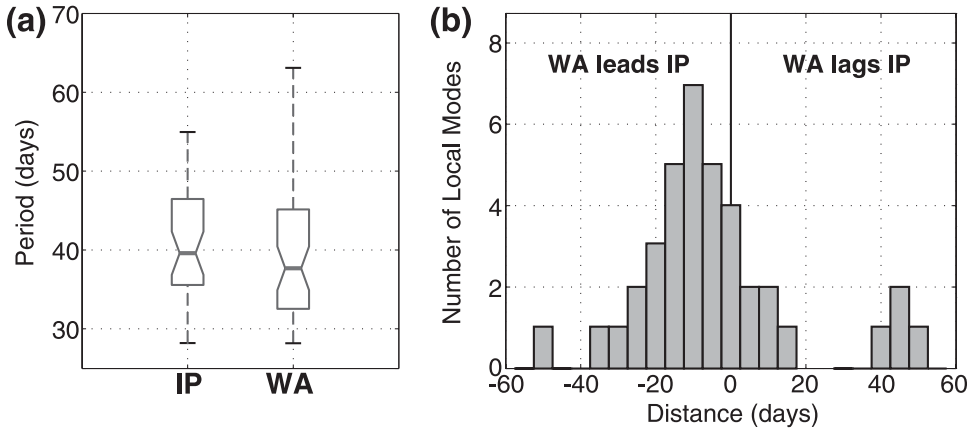

FIG. 4. (a) Box-and-whisker plot of the period (days) of the local modes of the WA and IP experiments. The boxes have lines at the lower quartile, median, and upper quartile values. The whiskers are lines extending from each end of the box to show the range of the data. (b) Histogram of the distance (days) between each local mode of the IP experiment and the closest local mode of the WA experiment.

The IP experiment demonstrates that the MJO has, on average, a significant impact on West African atmospheric convection; however, the amplitude of the OLR fluctuations remains rather weak. The WA experiment investigates whether the MJO is the only mode of atmospheric variability at the origin of the 40-day variability of the WAM.

The convective events extracted over West Africa are slightly shorter than the Madden–Julian perturbations described in the IP experiment (Fig. 4a). Their median value (38 days) is consistent with the findings of Janicot and Sultan (2001) and Sultan et al. (2003) concerning the WAM intraseasonal variability. Extreme values spread from 28 to 70 days, which is out of the 30–60-day range usually used to characterize the MJO, and show that the WAM is less periodic (or that its periodicities are more irregular) than the MJO. The mean propagative pattern (Fig. 3a) shows a clear standing component over the Gulf of Guinea and central Africa and a weak westward propagation over the Sahel, also found in Janicot et al. (2009). More importantly, the propagative patterns over the Indo-Pacific basin show very strong similarities with the IP experiment (Fig. 3b). The phase relationship between the two regions ($\pi/2$ rad; i.e., a quarter of cycle) and the relative amplitude of the OLR signals over the two areas are remarkably similar between the two experiments. Moreover, the local modes extracted in the WA experiment occur, on average, 3.1 days before those extracted in the IP experiment (Fig. 4b), and 70% of these occur less than 20 days (half a period; Fig. 4a) before or after a local mode extracted in the IP experiment. Consequently, it is concluded that a majority of the intraseasonal perturbations in the WAM are embedded in the larger-scale patterns of the MJO (Figs. 3, 4). Note that a substantial part of WA events (30%) lag IP events, which can be interpreted as MJO events initiated 20 to 30 days earlier over the Indian basin but followed by a period of weak intraseasonal activity.

What exact part of the 40-day fluctuations in the WAM region relate to the MJO? In other words, how many convective events recorded over West Africa are embedded in large-scale patterns that present high OLR amplitudes farther east and west? To answer this question, we calculated the mean amplitude of the OLR perturbations over the two regions of interest, IP and WA (Fig. 3). Thus, for each local mode and for both the WA and IP experiments, we obtain the amplitude for the OLR perturbations averaged over the WA and IP areas. Our aim here is to evaluate the number of local modes presenting high OLR amplitudes over both areas and those only energetic over one region.

The scatterplots intersecting the regional amplitude values are shown on Fig. 5. There is no significant relationship between the amplitude of the OLR fluctuations over the WA and IP regions according to a Bravais–Pearson test (95% level); that is, strong fluctuations over West Africa do not correspond to the strongest events in the Indian and west Pacific basins. All local modes appear to be more energetic over the IP region (with OLR amplitudes varying between 8 and 12 W m^{-2}, versus between 4 and 6 W m^{-2} over the WA region). These values are spatial means and can reach far higher values locally: this will be discussed in section 4.

This result, true for both experiments, is not surprising for the IP experiment because the local modes were detected over the area known to concentrate the strongest MJO signal (e.g., Matthews 2000). In the WA

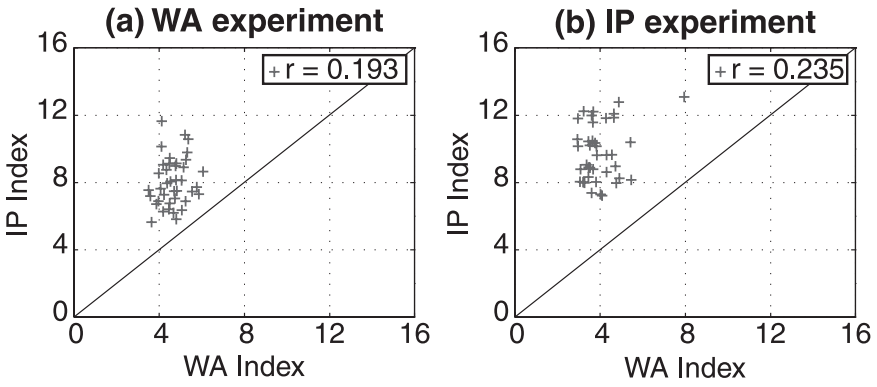

FIG. 5. Scatterplots intersecting the OLR amplitude (W m^{-2}) averaged over the two areas shown on Fig. 3 for the local modes of the (a) WA and (b) IP experiments. The linear correlation coefficient values are indicated.

experiment, it is more meaningful and it demonstrates that a majority of 40-day events extracted over Africa are of larger scale than the only WA domain and thus project onto stronger OLR perturbations over the Indo-Pacific basin. Hence, the 40-day variability in the WAM does not constitute a phenomenon intrinsic to the monsoon system but is mainly embedded in larger-scale (MJO) patterns.

The OLR amplitude over a given region is slightly higher over the area used to detect the local modes; that is, OLR fluctuations in WA are stronger in the WA experiment and those in the IP region are stronger in the IP experiment. This shows that the correspondence between the OLR perturbations over the two regions is not perfect; that is, local modes detected over the IP (WA) region project imperfectly over West Africa (the Indo-Pacific basin).

b. Amplitude of the convective perturbations

What are the parameters that influence the amplitude of the OLR perturbations over West Africa? In other words, are the strongest 40-day events in the WAM recorded during specific background climate conditions (note that Fig. 5 established that their amplitude is not related to the strength of the MJO perturbations over the warm pool)? To investigate this issue, Fig. 6 shows the composite anomalies of the tropical SST field between the strongest and the weakest local modes over both WA and IP regions and both experiments. These composites were formed using the 33rd and the 66th percentiles of the regional mean OLR amplitude.

In the IP experiment (Fig. 6b), the amplitude of the OLR perturbations over the Indo-Pacific basin is favored slightly by warm SST over this area—a result already found by Kessler (2001) over the central Pacific basin but never explicitly obtained over the Indian and west Pacific basins. Note, however, that the SST anomalies there remain rather weak. The strongest convective perturbations over West Africa occur during warm conditions in the central Pacific and cold conditions in the equatorial Atlantic basin. Isolated pockets of abnormally cold SST anomalies are also found in the west Pacific and the Arafura Sea, southwest of Papua New Guinea. This pattern is reminiscent of El Niño conditions, during which the warm pool is located farther east in the central Pacific basin. The cooling of the equatorial Atlantic Ocean is seen to be related to an increase of the surface wind stress caused by a strengthening of the trade winds (Fig. 8). Hence, we suggest that although atmospheric convection tends to be weakened during El Niño years in West Africa, it is more strongly modulated at the intraseasonal time scale by the MJO. A similar result was obtained over southern Africa by Pohl et al. (2007) during the austral summer season.

The SST anomaly patterns that are synchronous with the local modes extracted in the WA experiment are slightly different. The strongest events in the IP area do not occur during significantly different SST conditions than the weakest ones, except for an ambiguous pocket of negative SST anomalies (i.e., cold SST values during the strongest Madden–Julian events over the IP region) located in the Caribbean Sea and western Atlantic basin between 10° and 20°N. More interestingly, the strongest OLR perturbations over West Africa are unambiguously concomitant with warm conditions in the overall tropical belt, especially over the Indian basin. Coherent signals are also found in the southern Pacific and Atlantic basins. Note the strong anomalies (+1.5°C) in the Gulf of Guinea and along the Benguela coast. Surface conditions might be a key parameter to explain the amplitude of the intraseasonal oscillations in the WAM.

Figure 7 depicts the associated atmospheric anomalies by presenting the composite velocity potential anomalies between these same groups of events. Figure 8 shows the

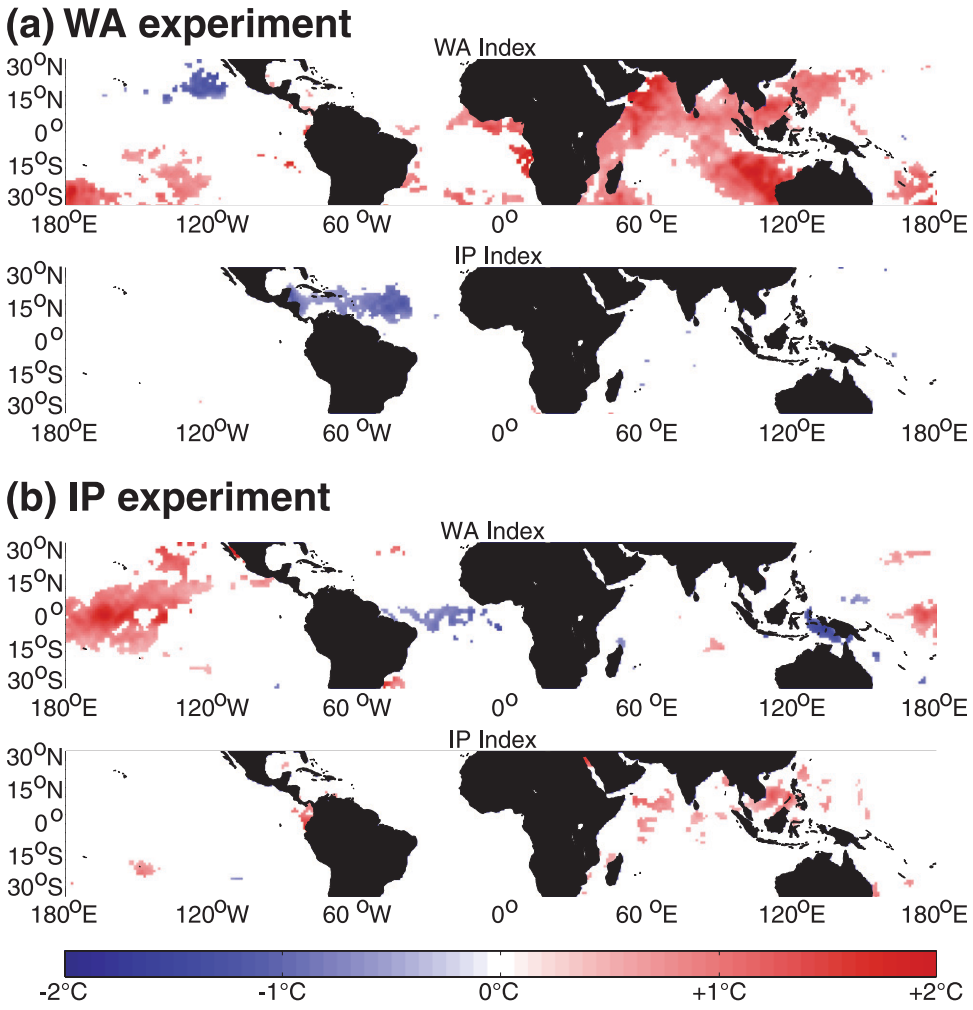

FIG. 6. Difference of synchronous SST (°C) between the local modes associated with the strongest and the weakest OLR amplitude averaged in the (top) WA and (bottom) IP regions for the (a) WA and (b) IP experiments. Differences that are not significant (two-tailed *t* test; 95% level) are shaded white. See legend for color shading.

composite anomalies of zonal and vertical wind at the low latitudes. In both experiments, the strongest modes over the WA region occur when anomalously strong subsiding motion prevails in the troposphere over Africa. The signals are continuously significant from the surface to 400 hPa. In accordance with the synchronous SST anomalies (Fig. 6), ascending motion prevails over the Indian (central Pacific) basin during the strongest modes of the WA (IP) experiment (i.e., over the regions showing positive temperature anomalies). Lower-layer convergence and upper-level divergence is also found over these areas (Figs. 7, 8). It is thus suggested that the amplitude of the intraseasonal oscillations in West Africa could relate to a Walker-type circulation, with subsiding anomalies over the region favoring strong convective fluctuations. Our patterns are consistent with the discussion between Semazzi et al. (1988, 1989) and Khandekar (1989) concerning the implication of the Walker-type circulation, and also with associated SST anomalies in the occurrences of seasonal droughts in sub-Saharan Africa. Zonal wind anomalies are of opposite sign between the lower and the upper layers of the troposphere at almost all longitudes (Fig. 8), although their amplitude is rather weak. Ascending motion also remains small over the Pacific, in spite of coherent signals in the velocity potential at 850 and 200 hPa. In contrast, horizontal wind signals are weak over Africa but vertical velocity anomalies are remarkably strong. Additional analyses (not shown) reveal that the strongest atmospheric signals in the vertical velocity are restricted to the equatorial latitudes. Besides, the monsoon flow itself does not present any significant signal.

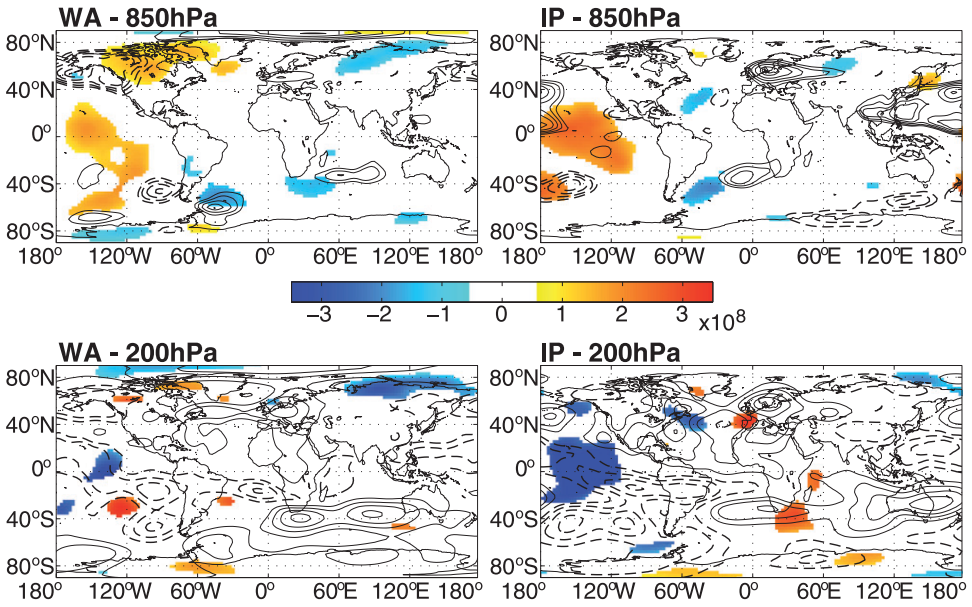

FIG. 7. Composite velocity potential (shading) and streamfunction (contours) anomalies between the local modes associated with the strongest and the weakest OLR amplitudes averaged in the WA region for the (left) WA and (right) IP experiments. Velocity potential anomalies that are not significant according to a *t* test at the 95% level are shaded white. Solid (dashed) contours denote positive (negative) streamfunction anomalies. Contour interval is 8×10^8 m^2 s^{-1}.

At the intraseasonal time scale, one hypothesis to relate the amplitude of MJO-associated perturbations to these atmospheric and surface configurations could be that the phase of suppressed rainfall and convection is stronger and/or more persistent when background subsiding conditions prevail. This suggests that the dry phase could be associated with stronger anomalies than the enhanced convection phase. This issue is investigated in section 4.

4. OLR and rainfall composite anomalies

a. Average MJO life cycle over West Africa

Section 3 showed that a large majority of the 40-day convective perturbations in the WAM are primarily related to the MJO activity in the tropics. Hence, it is possible to use global-scale MJO descriptors to focus on the phase locking between the West African rain and OLR fluctuations and the MJO. We also aim here at quantifying the consequences of the latter on the daily rainfall amounts. We use the global MJO indices developed by WH04 to perform composite analyses over the MJO life cycle. All the fields presented in this section were not filtered prior to the computation of the composites.

Figure 9 presents the composite OLR anomalies for the eight phases of the MJO identified in WH04. The results are slightly different from those of Matthews (2004), who used a regional MJO index based only on the OLR field. We find here a predominant dry phase (MJO phases 0–π) with no clear propagation of the suppressed convection patterns over Africa. The signals are both highly significant and spatially coherent. On the contrary, phases π–$7\pi/4$ show negative OLR anomalies (i.e., enhanced convection over the region). Note, however, that these wet phases show anomalies of smaller amplitude: up to -5 W m^{-2} compared to $+10$ W m^{-2} during the dry phase. Although the regional mean amplitude of the OLR fluctuations is 4 W m^{-2} (Fig. 5), these values reach higher values in some regions (grid points), suggesting a potential influence on daily rainfall. The spatial consistency of the negative anomalies is also weaker, and the most energetic signals of enhanced convection are mostly recorded over the Gulf of Guinea seashore (i.e., in the south of the ITCZ during this season of the year and in agreement with Fig. 3). The Sahel is only influenced by the dry phase of the MJO because the wet phase is not associated with significant signals there, except for the eastern Sahel (east of Lake Chad) during phases $3\pi/2$–$7\pi/4$.

The strongest positive OLR anomalies are concentrated in the 0–$\pi/2$ quadrant (Fig. 9); that is, when the large-scale convective clusters associated with the MJO are located over the west Pacific basin and northern India (see WH04, their Fig. 11). At this time of the intraseasonal pseudocycle, suppressed convection extends

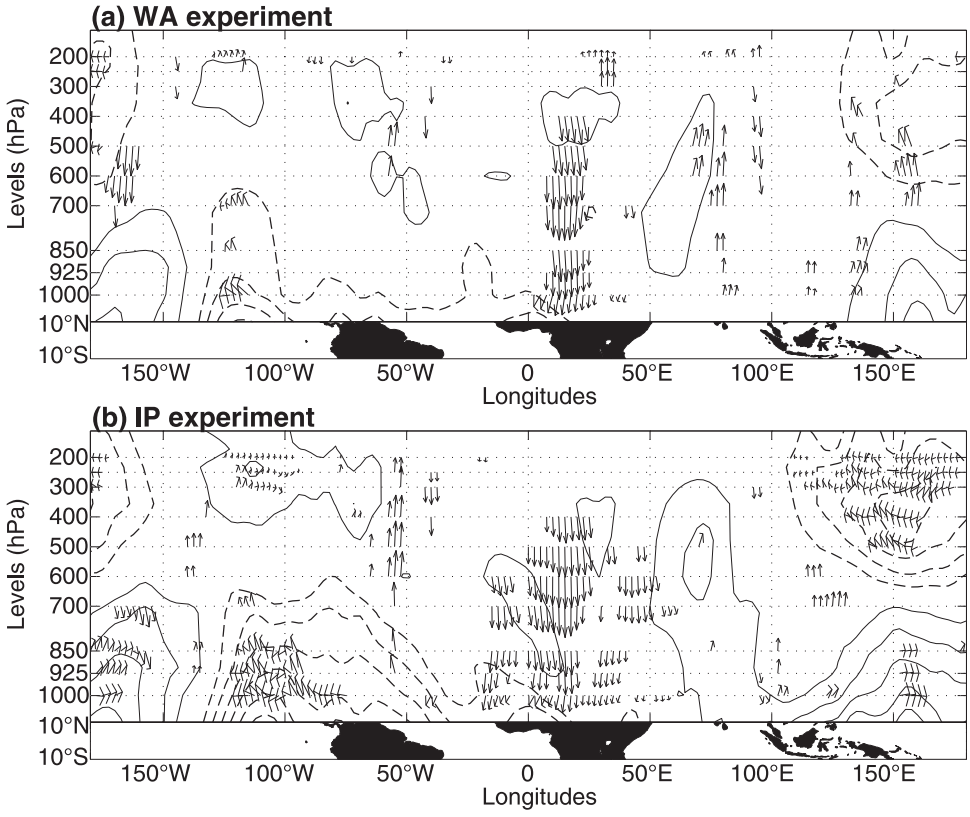

FIG. 8. Vertical section of the troposphere representing the difference of synchronous atmospheric circulation averaged between 10°N and 10°S between the local modes associated with the strongest and the weakest OLR amplitude averaged in the WA region for the (a) WA and (b) IP experiments. The zonal and vertical components of the wind were normalized prior to the analysis for homogeneity. Only significant anomalies (two-tailed Hotelling t^2 test; 95% level) are shown. Contours indicate the difference in the synchronous zonal wind. Solid (dashed) lines correspond to westerly (easterly) anomalies. Contour interval is 0.5 m s^{-1} with the first contour at 0.5 m s^{-1}.

from tropical Africa to the southern Indian basin. This result confirms the in-phase OLR fluctuations depicted by both the WA and IP experiments in Fig. 3. Enhanced convection mostly occurs over West Africa between π and $3\pi/2$; that is, one-eighth of the cycle (5–6 days) before the onset of convection over the Indian Ocean (WH04). Negative OLR anomalies over West Africa are preceded by enhanced convection over the Americas and are followed by the development of the large-scale ''convective superclusters'' (Madden and Julian 1994) over the equatorial Indian Ocean. Thus, they appear to be embedded in the eastward propagation of convective anomalies along the equator, consistent with Fig. 3, and remain bounded in the equatorial latitudes. Therefore, they mostly affect the Guinean belt and barely concern the monsoon flow located farther north. Consequently, the dry (suppressed convection) phase of the MJO is of larger importance for the Sahel region than the equatorially trapped negative OLR signals.

b. Consequences for rainfall variability

To confirm these findings, we apply the same methodology on daily rainfall records. This study constitutes the first attempt to use in situ rain gauge records (see Fig. 1) to evaluate the incidence of the MJO on West African rainfall variability. Their use makes it possible to assess whether the OLR dataset is an accurate proxy for the rain over the area, as far as intraseasonal activity is concerned.

Homogeneous rainfall indices are first obtained through a principal component analysis (PCA) with a varimax rotation, based on the correlation matrix, and applied to the rainfall time series on the JAS period after removal of the annual cycle. Because the distribution of the daily amounts is not Gaussian, we used the square root of the rain as input data for the PCA. The first three PCs, significant according to a scree test and explaining 25% of the overall original variance, were retained and then rotated, providing three homogeneous indices. Each rainfall

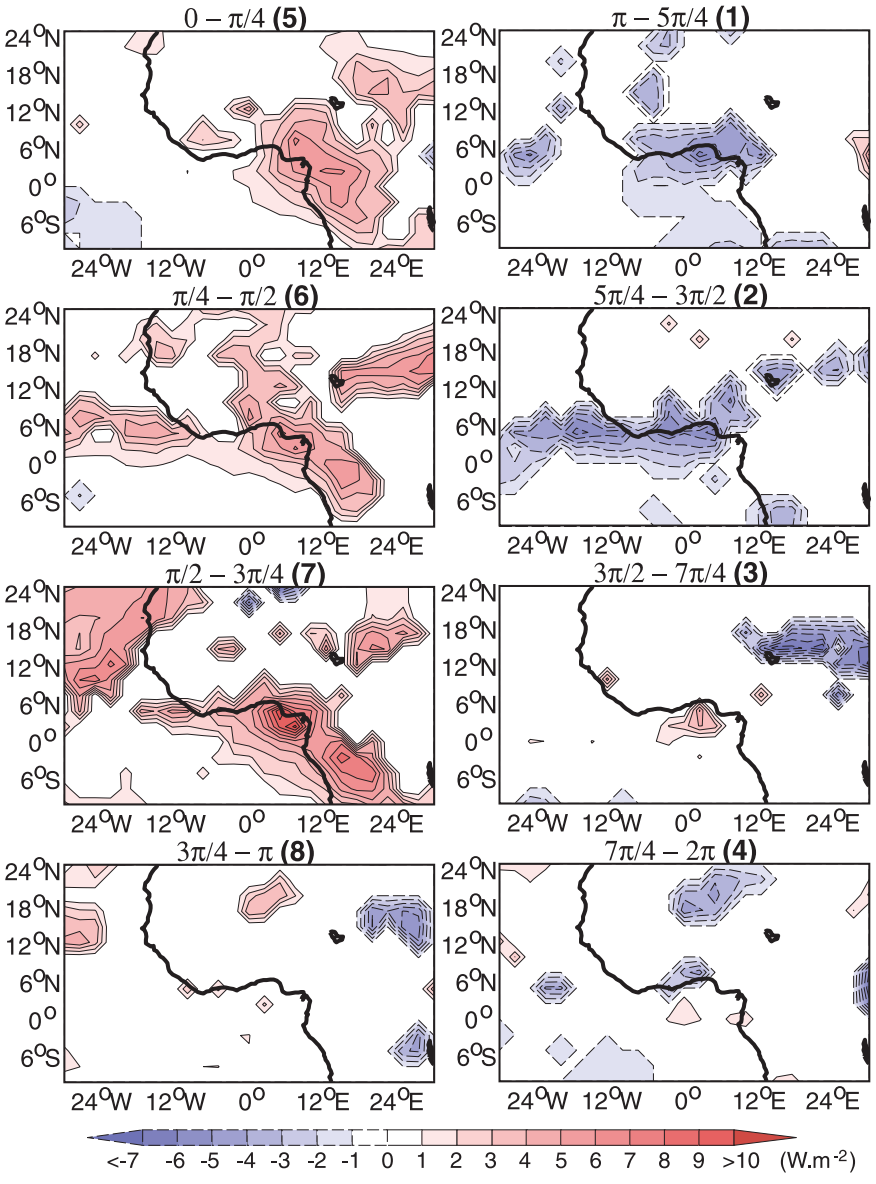

FIG. 9. Composite maps of unfiltered OLR anomalies (W m^{-2}) after removal of the annual cycle and for the eight phases of the MJO defined in WH04. Period of study: JAS 1979–2007. Anomalies that are not significant (*t* test; 95% level) are shaded white; significant positive (negative) anomalies appear in red (blue) and are black contoured with solid (dashed) lines. Contour interval is 1 W m^{-2}; see legend for color shading.

index is then constituted as the average rainfall amount for the stations affiliated with this index [i.e., significantly correlated with the score time series of the rotated principal component (RPC)]. Missing values (Fig. 1) were excluded from the analyses. We finally obtained three time series (expressed in millimeters per day) and solved the problem of the constraint of orthogonality. Analysis of their associated time series allows insight into the spatial coherence of the Sahel at the MJO time scale.

The locations of the three rainfall indices are shown in Fig. 10 (left). The associated time series are then composited over the MJO life cycle (Fig. 10a; i.e., against the eight phases of the MJO already used in Fig. 9). In accordance with OLR anomalies, phases 0–π are responsible for the most important rainfall departures and show persistent dry conditions. On the contrary, phases π–2π are associated with weaker and less persistent wet anomalies. Both amplitude and persistence indicate that

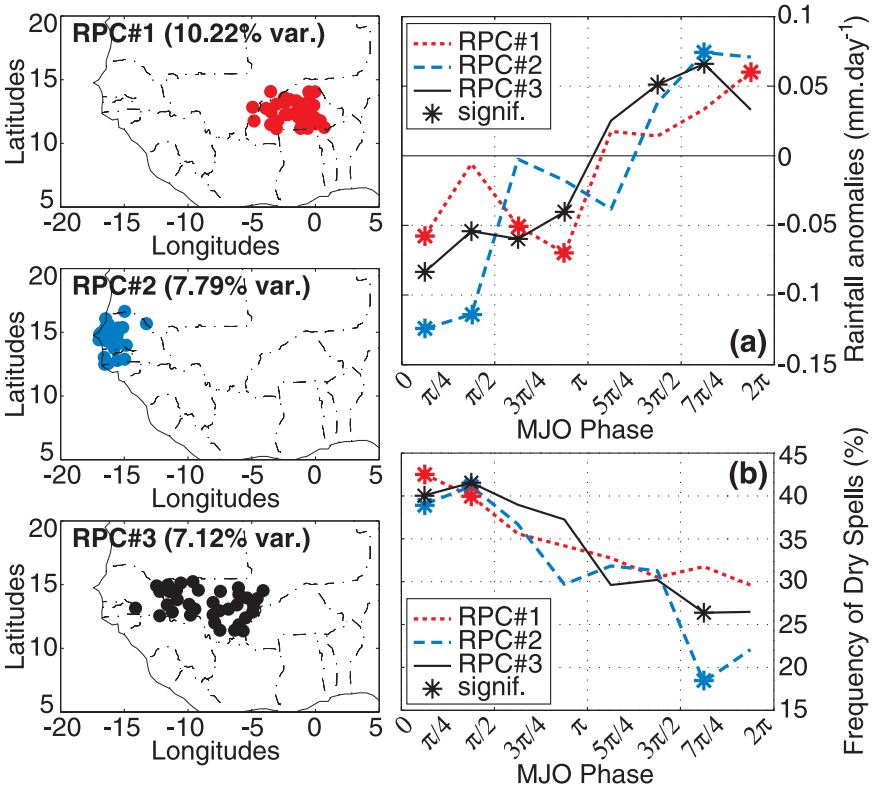

FIG. 10. (left) Location of the rain gauge stations constituting the three rainfall indexes obtained through a PCA with a varimax rotation (see text for details). (right), (a) Composite analysis of the daily rainfall amounts (mm day^{-1}) in the three indexes against the phases of the MJO. Asterisks denote significant anomalies according to a *t* test (95% level). (b) Frequency of the dry spells (%) for the different phases of the MJO (see text for details). Asterisks denote significantly higher or lower probabilities compared to the seasonal mean probability of occurrence (*t* test; 95% level).

the dry phase of the MJO is predominant over the Sahel during the monsoon, although both dry and wet anomalies are significant according to a *t* test. Note also that the eight phases discriminate the overall variance of the three time series, denoting a significant influence of the MJO on the WAM. These results are nonetheless obtained for a rather short period (JAS 1979–90; i.e., 12 rainy seasons, constituting a total of 1104 days included in the analysis). To ensure that the sample size is large enough to provide robust results, we also used the daily MJO indices developed by Pohl and Matthews (2007) over the 1948–2006 period and found very similar rainfall anomalies. Hence, the significance of the results is not imputable to the sample size.

However, the amplitude of rainfall anomalies (Fig. 10a) is very weak, which could be attributed to the fact that we considered regional rainfall indices only. To assess the spatial coherence of these signals and to have a closer scrutiny to their potential impacts on agriculture, we defined a dry spell as a rainfall threshold of 1 mm day^{-1} (Diop 1999) recorded in more than 50% of the stations within each index shown in the left panels of Fig. 10. Dry spells can be at the origin of dramatic decrease in agriculture production (Sivakumar 1992; Barron et al. 2003). Given the predominance of the dry phase over the MJO cycle (Figs. 9, 10a), one can hypothesize that the probability and/or the length of such dry spells is significantly modulated by the MJO.

The frequency of the dry spells during the eight different MJO phases is shown in Fig. 10b. Consistent with rainfall anomalies (Fig. 10a), MJO phases 0–π are associated with dry conditions and a relatively high probability for dry spells to occur (especially during the 0–π/2 quadrant). On the contrary, the π–2π half cycle shows a slightly (and barely significant) decreased probability for the dry spells. The probability of occurrence is indeed not significantly reduced for RPC1, a rainfall index describing the rainfall field over Burkina Faso, which denotes the relative weakness of the wet phase of the MJO over the region. Note that the eight phases of the intraseasonal cycle significantly discriminate the probability of the dry spells for the three rainfall indices,

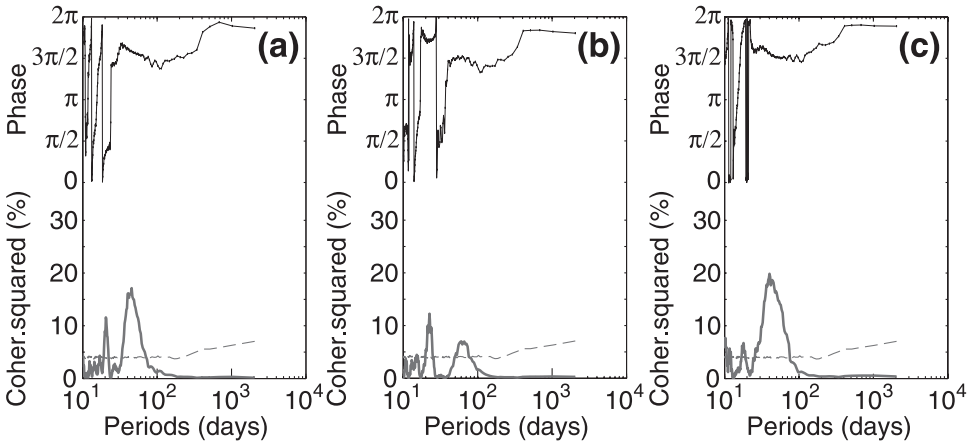

FIG. 11. Cross-spectrum analysis of the rainfall index described by the MJO index RMM1 defined in WH04, along with (a) RPC1, (b) RPC2, and (c) RPC3. Analyses are carried out on normalized data for the JAS 1979–90 period, with other months padded with zeros. Gray lines are square coherence. Dashed lines indicate the 95% level according to 1000 random time series obtained as permutations of the original time series and having the same lag-1 serial correlation. Solid black line with plus signs denotes the phase relationship in radians.

demonstrating again the significance of the influence of the MJO on West African rainfall. From these results, one can conclude (i) that the dry phase is clearly predominant and (ii) that the rainfall anomalies associated with the MJO present a good spatial coherence and affect the overall Sahel region.

What is the part of the variance of the in situ rainfall records that is related to global-scale MJO activity? To quantify the influence of the latter on the intraseasonal rainfall variability over the western Sahel, we performed cross-spectrum analyses between the three rainfall indexes (Fig. 10) and the RMM1 time series, which was computed by WH04 and used here as a single descriptor of the MJO activity. The results are shown in Fig. 11. Note that the same results are obtained with RMM2 but with a phase relationship shifted by $\pi/2$ radians. Once again, very similar results are obtained for the overall 1950–90 period using the MJO indices computed by Pohl and Matthews (2007).

In the 30–60-day range, the common variance between the MJO index and the rainfall time series peaks at 20% for the RPC1 and RPC3 indexes and is highly significant, according to the random simulations. Though still significant, the common variance with RPC2 is smaller (7% only). These values are lower than those of Maloney and Shaman (2008), who estimated that the MJO explains about 30% of 30–90-day precipitation (as estimated by the TRMM dataset) variance in the West African monsoon region. The phase relationship between the RMM1 time series and the three regional indices is constant for the intraseasonal frequencies (values centered on $3\pi/2$ for the three regions), confirming that the MJO-associated anomalies in the rain occur in phase over the Sahel. The weakness of the results for the RPC2 time series (Senegal; Fig. 10) suggests an increasing influence of the MJO toward the east; Pohl and Camberlin (2006a,b) pointed out stronger associations between the oscillation and rainfall variability over East Africa and particularly over the African Highlands. Although its influence is significant on the West African atmospheric convection (Figs. 3, 9; see also Matthews 2004) and rainfall (Figs. 10, 11), the MJO thus remains a partial forcing during the WAM that triggers a somewhat small part of the overall climate intraseasonal fluctuations. Even if the 40-day variability over West Africa was shown to be basically related to the near-global scale MJO, both lower and shorter frequencies strongly interfere with it.

5. Conclusions and discussion

This study helps to document the implication of the Madden–Julian oscillation (MJO) in the 40-day variability of the West African monsoon (WAM). Based on a local mode analysis, we extracted the intraseasonal perturbations in the atmospheric convection over the ''core'' region of the MJO, namely the Indian and west Pacific basins. We then projected these events over a larger domain and showed that the MJO convective perturbations over the Indian and west Pacific Oceans are generally preceded by weak convective signals over West Africa (4–6 W m^{-2}, on average).

In reverse, we specifically extracted the 40-day fluctuations of the WAM area and projected these events over a larger area, including the Indo-Pacific warm pool

region. The intraseasonal perturbations in the WAM project were symmetrically extracted onto convective perturbations of larger amplitude over the Indo-Pacific region, confirming that they are embedded in patterns of larger scale than the African sector alone. The propagative patterns of the associated anomalies over the Indian and Pacific basins are clearly reminiscent of the boreal summer MJO, because northward (westward) propagations are found over the Indian (west Pacific) longitudes. Hence, we demonstrated that most 40-day convective perturbations in the WAM are embedded in the MJO large-scale patterns.

Interestingly, the amplitude of the OLR fluctuations over West Africa is not directly related to that of the convective perturbation over the warm pool region. Strong convective events over the Indian basin do not necessarily induce strong OLR signals in the WAM. The amplitude of the 40-day events over West Africa seems, on the contrary, to be closely related to the background climate conditions, especially changes in the vertical velocity at the equatorial latitudes. Strong modulations of the convection over West Africa associated with the MJO occur with subsiding anomalies over Africa and ascending modulations occur over the Indo-Pacific basin, where positive SST anomalies, lower-layer convergence, and upper-layer divergence are also prevalent. These anomaly patterns suggest the implication of a Walker-type zonal circulation at the very low latitudes.

The influence of subsiding motion in the troposphere on regional intraseasonal activity could be through the dry phase of the MJO, hypothesized to be stronger than the wet phase. To verify this, composite analyses of OLR and in situ rainfall records are used to document the average MJO life cycle and associated anomalies over West Africa, and they are also used to assess the role of the dry phase of the MJO. Negative OLR signals (i.e., enhanced atmospheric convection anomalies) are indeed restricted to the very low latitudes of the Gulf of Guinea and barely reach the Sahel. On the contrary, positive OLR anomalies show stronger persistence and amplitude (locally reaching $+10\,\mathrm{W\,m^{-2}}$ versus $-5\,\mathrm{W\,m^{-2}}$ for the convective phase) and are spatially more coherent, especially at the latitude of the Sahel. These findings, reinforced by similar conclusions in rain gauge records, confirm that the dry phase is predominant over West Africa. Background subsiding motion and the dry phase of the MJO add their effects and favor strong suppressed convection conditions at the regional scale, which induces intraseasonal perturbations of particularly high amplitude.

The consequences for regional rainfall variability are further examined using 118 rain gauge stations located in the western and central Sahel. Three homogeneous regional indices depicting the rainfall field over Senegal, Mali, and Burkina Faso are obtained through a principal component analysis with a varimax rotation. Given the predominance of the dry (suppressed convection) phase over these latitudes, we explored the implication of the MJO in the frequency of dry spells during the monsoon season. The latter are defined as daily rainfall amounts less than 1 mm recorded in at least 50% of the rain gauge stations constituting each regional index. The results are highly significant and denote a strong implication of the MJO in the occurrences of dry phases within the rainy season. Although the amplitude of the associated OLR perturbations is moderate, the MJO appears as an important atmospheric forcing that triggers a significant part of the temporal distribution of the rain during the monsoon. Cross-spectrum analyses estimated, however, that 9%–20% of the rainfall intraseasonal variance is related to the MJO activity in the tropics, indicating that other phenomena strongly interfere with its signal. In other words, although the 40-day variability over West Africa mainly relates to the MJO, it explains only a limited part of the overall variability at the subseasonal scales, interfered with by both higher- and lower-frequency noise.

The local mode analysis additionally provided a powerful tool to investigate the propagative properties of the large-scale convective clusters associated with the MJO and 40-day fluctuations of the WAM over the African continent. Two distinct patterns were identified: (i) a standing component over the Gulf of Guinea that is restricted to the very low latitudes in both hemispheres, preceded by convective signals over Amazonia and followed by large-scale northward-propagating clusters over the Indian basin (this convective signal is thus embedded in the well-known eastward propagation of the MJO in the tropics); and (ii) rather slow propagations toward the west at the northern tropical latitudes linked to Rossby waves and consistent with Matthews (2004) and Janicot et al. (2009). Positive OLR anomalies are seen to propagate from the central Indian Ocean to the East African Highlands, the Sahel, and then the Senegalese coast. Their spatial coherence and extension and their amplitude are larger than the equatorially trapped negative OLR signals propagating eastward. Given the phase locking between these propagations and the global-scale MJO activity, we hypothesize that the enhanced convection phase is associated with the large-scale instability associated with the MJO in the tropical belt. The westward propagation of suppressed convection over the Sahel is, on the contrary, caused by the atmospheric Rossby wave generated over the Indian basin by the convective onset of the MJO there.

Contrary to the eastward-propagating convective clusters, suppressed convection associated with the atmospheric Rossby wave is not restricted to the equatorial rail and therefore forms the predominant signature of the MJO over the Sahel.

This might explain why high amplitudes in the intraseasonal convective signal over West Africa seem to be related to the specific regional Walker-type circulation and positive sea surface temperature anomalies over the Indian basin. On one hand, under anomalously warm conditions in the west Pacific, the eastward-propagating component of the MJO extends farther east over the central Pacific (Kessler 2001). The signal is thought to reach equatorial Africa, whereas it usually decays over the American and Atlantic sectors. More importantly for West Africa, we may expect that the westward-propagating Rossby component of the MJO, which forms the predominant signature of the MJO over the Sahel, will be more active and at the origin of a predominant dry phase when background subsiding motion prevails in the troposphere over Africa. These two factors could contribute to enhance the amplitude of the MJO-associated convective anomalies in the WAM.

A set of numerical experiments is needed to validate these hypotheses. The specific influence of warm SST anomalies in the Indo-Pacific basin on the MJO and its effects on the WAM need to be addressed. Similarly, the incidence of modifications in the Walker-type circulation and in the vertical wind shear must be clarified. Based on a GCM, we aim at investigating the role of these background climate conditions on the propagation of intraseasonal signals and associated convective variability over West Africa. We particularly plan to investigate the respective influence of these surface and atmospheric configurations on both eastward- and westward-propagating components of the intraseasonal oscillation.

Acknowledgments. Based on French initiative, AMMA was built by an international scientific group and is currently funded by a large number of agencies, especially from France, the United Kingdom, the United States, and Africa. It has been the beneficiary of a major financial contribution from the European Community's Sixth Framework Research Programme. (Detailed information on scientific coordination and funding is available online at the AMMA International Web site at http://www.amma-international.org.) We acknowledge the FRIEND-AOC group for providing us with the rainfall data. B. P. thanks Jean-Philippe Duvel (LMD/ENS, Paris, France) for the scripts of the LMA and Daniel Nethery for his test to suppress overlapping local modes. Three anonymous reviewers greatly helped improve the manuscript.

REFERENCES

Anderson, J. R., D. E. Stevens, and P. R. Julian, 1984: Temporal variations of the tropical 40–50-day oscillation. *Mon. Wea. Rev.,* **112,** 2431–2438.

Annamalai, H., and J. M. Slingo, 2001: Active/break cycles: Diagnosis of the intraseasonal variability of the Asian summer monsoon. *Climate Dyn.,* **18,** 85–102.

Anyamba, E. K., and B. C. Weare, 1995: Temporal variability of the 40-50-day oscillation in tropical convection. *Int. J. Climatol.,* **15,** 379–402.

Barron, J., J. Rockstrom, F. Gichuki, and N. Hatibu, 2003: Dry spell analysis and maize yields for two semi-arid locations in East Africa. *Agric. For. Meteor.,* **117,** 23–37.

Bellenger, H., and J.-P. Duvel, 2007: Intraseasonal convective perturbations related to the seasonal march of the Indo-Pacific monsoons. *J. Climate,* **20,** 2853–2863.

Carvalho, L. M. V., C. Jones, and B. Liebmann, 2004: The South Atlantic convergence zone: Intensity, form, persistence, and relationships with intraseasonal to interannual activity and extreme rainfall. *J. Climate,* **17,** 88–108.

Diop, M., 1999: Caractérisation du facteur hydrique en agriculture pluviale au Sénégal: le cas de l'arachide et du mil. Ph.D. thesis, Université de Bourgogne, 185 pp.

Duvel, J.-P., and J. Vialard, 2007: Climatology of sea surface temperature perturbations associated with the Madden–Julian oscillation. *J. Climate,* **20,** 3056–3082.

——, R. Roca, and J. Vialard, 2004: Ocean mixed layer temperature variations induced by intraseasonal convective perturbations over the Indian Ocean. *J. Atmos. Sci.,* **61,** 1004–1023.

Foltz, G. R., and M. J. McPhaden, 2004: The 30–70 day oscillations in the tropical Atlantic. *Geophys. Res. Lett.,* **31,** L15205, doi:10.1029/2004GL020023.

Goulet, L., and J.-P. Duvel, 2000: A new approach to detect and characterize intermittent atmospheric oscillations: Application to the intraseasonal oscillations. *J. Atmos. Sci.,* **57,** 2397–2416.

Gray, B. M., 1988: Seasonal frequency variations in the 40-50 day oscillation. *Int. J. Climatol.,* **8,** 511–519.

Hsu, H.-H., and C.-H. Weng, 2001: Northwestward propagation of the intraseasonal oscillation in the western North Pacific during the boreal summer: Structure and mechanisms. *J. Climate,* **14,** 3834–3850.

Janicot, S., and B. Sultan, 2001: Intra-seasonal modulation of convection in the West African monsoon. *Geophys. Res. Lett.,* **28,** 523–526.

——, F. Mounier, N. M. J. Hall, S. Leroux, B. Sultan, and G. N. Kiladis, 2009: The dynamics of the West African monsoon. Part IV: Analysis of the 25–90-day variability of convection and the role of the Indian monsoon. *J. Climate,* **22,** 1541–1565.

Kanamitsu, M., W. Ebisuzaki, J. Woollen, S.-K. Yang, J. J. Hnilo, M. Fiorino, and G. L. Potter, 2002: NCEP–DOE AMIP II reanalysis (R-2). *Bull. Amer. Meteor. Soc.,* **83,** 1631–1643.

Kessler, W. S., 2001: EOF representation of the Madden–Julian oscillation and its connection with ENSO. *J. Climate,* **14,** 3055–3061.

Khandekar, M. L., 1989: Comments on ''An investigation of the relationship between sub-Saharan rainfall and global sea surface temperatures.'' *Atmos.–Ocean,* **27,** 597–600.

Knutson, T. R., and K. M. Weickmann, 1987: 30–60-day atmospheric oscillations: Composite life cycles of convection and circulation anomalies. *Mon. Wea. Rev.,* **115,** 1407–1436.

Lawrence, D. M., and P. J. Webster, 2002: The boreal summer intraseasonal oscillation: Relationship between northward and eastward movement of convection. *J. Atmos. Sci.,* **59,** 1593–1606.

Liebmann, B., and C. A. Smith, 1996: Description of a complete (interpolated) outgoing longwave radiation dataset. *Bull. Amer. Meteor. Soc.,* **77,** 1275–1277.

Madden, R. A., 1986: Seasonal variations of the 40–50-day oscillation in the tropics. *J. Atmos. Sci.,* **43,** 3138–3158.

——, and P. R. Julian, 1994: Observations of the 40–50-day tropical oscillation—A review. *Mon. Wea. Rev.,* **122,** 814–837.

Maloney, E. D., and J. T. Kiehl, 2002: MJO-related SST variations over the tropical eastern Pacific during Northern Hemisphere summer. *J. Climate,* **15,** 675–689.

——, and J. Shaman, 2008: Intraseasonal variability of the West African monsoon and Atlantic ITCZ. *J. Climate,* **21,** 2898–2918.

Matthews, A. J., 2000: Propagating mechanisms for the Madden-Julian oscillation. *Quart. J. Roy. Meteor. Soc.,* **126,** 2637–2652.

——, 2004: Intraseasonal variability over tropical Africa during northern summer. *J. Climate,* **17,** 2427–2440.

Mounier, F., 2005: La variabilité intra-saisonnière de la mousson de l'Afrique de l'Ouest et Centrale. Ph.D. thesis, Ecole Polytechnique, 270 pp.

Pohl, B., and P. Camberlin, 2006a: Influence of the Madden-Julian oscillation on East African rainfall. Part I: Intraseasonal variability and regional dependency. *Quart. J. Roy. Meteor. Soc.,* **132,** 2521–2539.

——, and ——, 2006b: Influence of the Madden-Julian oscillation on East African rainfall. Part II: March-May season extremes and interannual variability. *Quart. J. Roy. Meteor. Soc.,* **132,** 2541–2558.

——, and A. J. Matthews, 2007: Observed changes in the lifetime and amplitude of the Madden–Julian oscillation associated with interannual ENSO sea surface temperature anomalies. *J. Climate,* **20,** 2659–2674.

——, Y. Richard, and N. Fauchereau, 2007: Influence of the Madden–Julian oscillation on southern African summer rainfall. *J. Climate,* **20,** 4227–4242.

Reynolds, R. W., N. A. Rayner, T. M. Smith, D. C. Stokes, and W. Wang, 2002: An improved in situ and satellite SST analysis for climate. *J. Climate,* **15,** 1609–1625.

Salby, M. L., and H. H. Hendon, 1994: Intraseasonal behavior of clouds, temperature, and motion in the tropics. *J. Atmos. Sci.,* **51,** 2207–2224.

Semazzi, F. H. M., V. Mehta, and Y. C. Sud, 1988: An investigation of the relationship between sub-Saharan rainfall and global sea surface temperatures. *Atmos.–Ocean,* **26,** 118–138.

——, ——, and ——, 1989: Reply to comments on ''An investigation of the relationship between sub-Saharan rainfall and global sea surface temperatures.'' *Atmos.–Ocean,* **27,** 601–605.

Sivakumar, M. V. K., 1992: Empirical analysis of dry spells for agricultural applications in West Africa. *J. Climate,* **5,** 532–539.

Sultan, B., S. Janicot, and A. Diedhiou, 2003: The West African monsoon dynamics. Part I: Documentation of intraseasonal variability. *J. Climate,* **16,** 3389–3406.

Wang, B., and X. Xie, 1997: A model for the boreal summer intraseasonal oscillations. *J. Atmos. Sci.,* **54,** 72–86.

Wheeler, M. C., and H. H. Hendon, 2004: An all-season real-time multivariate MJO index: Development of an index for monitoring and prediction. *Mon. Wea. Rev.,* **132,** 1917–1932.

Wu, M.-L. C., S. D. Schubert, M. J. Suarez, P. J. Pegion, and D. E. Waliser, 2006: Seasonality and meridional propagation of the MJO. *J. Climate,* **19,** 1901–1921.

Yasunari, T., 1980: A quasi-stationary appearance of the 30-40-day period in cloudiness fluctuations during the summer monsoon over India. *J. Meteor. Soc. Japan,* **58,** 223–229.

Zhang, C., 2005: Madden-Julian oscillation. *Rev. Geophys.,* **43,** RG2003, doi:10.1029/2004RG000158.